



In vivo and *in silico* Antifungal Activity of Cinnamon Leaf Oil and Lemongrass Oil containing Chitosan Microcapsules against *Aspergillus flavus*

P.G.J.D. KUMARATHUNGA¹, S. CHATHURANGI¹, R.P.S.P. RAJAPAKSHA¹, A.M.S.C. SOORIYAWANSHA¹, P.A.S.N.P. JAYAWARDENA¹, P.D.H. DANANJAYA¹, M.D.N. ALWIS¹, C.C. KADIGAMUWA¹, J.N. DAHANAYAKE¹ and S.R. WICKRAMARACHCHI^{1*}

Department of Chemistry, University of Kelaniya, Dalugama, Kelaniya, Sri Lanka

*Corresponding author: E-mail: suranga@kln.ac.lk

Received: 15 April 2024;

Accepted: 30 May 2024;

Published online: 29 June 2024;

AJC-21683

This study aimed to examine the potentiality of microencapsulated cinnamon leaf oil (CNO-CS-MCs) and lemongrass oil (LGO-CS-MCs) as natural fungicides against *Aspergillus flavus*. Oil encapsulated microcapsules were synthesized using ionotropic gelation method. Cinnamon leaf oil (CNO) and lemongrass oil (LGO) were characterized using GC-MS. *A. flavus* was isolated and identified using DNA sequencing. The minimum inhibitory and minimum lethal doses of oil-loaded microcapsules against *A. flavus* were evaluated under *in vivo* conditions and the results were further confirmed by *in silico* analysis. The major constituents of CNO and LGO were eugenol and citral, respectively. The minimum inhibitory doses of CNO-CS-MCs and LGO-CS-MCs were 5 mg and 7.5 mg, respectively. The minimum lethal dose of CNO-CS-MCs was 12.5 mg. As CNO showed considerably high antifungal activity than LGO, Computational investigations were carried out on the action of CNO against *A. flavus*. The highest protein-ligand interaction was observed for squalene epoxidase (SQ)-benzyl benzoate (BEN) complex with the binding energy of -7.70 kcal/mol. Molecular dynamics simulations were performed on SQ-BEN complex for 10 ns using CHARMM36 force field. The Rg, RMSD and RMSF results indicated the stabilization of the SQ-BEN complex throughout the simulation time.

Keywords: *Aspergillus flavus*, Chitosan, Cinnamon leaf oil, Lemongrass oil, Microcapsules.

INTRODUCTION

Rice stands as the most important crop, covering 34% (0.77/million ha) of Sri Lanka's total cultivated lands. Since the production of rice is seasonal, the excess production needs to be stored to fulfil the rice requirement during the off-season. In Sri Lanka, approximately 4-6% of the paddy production is lost during the storage period [1]. Since rice grains are a good substrate for storage fungi, rice is susceptible to a wide range of fungal species. Fungal infection of rice during storage is not only cause to reduce quality and economic value, but also responsible for producing harmful effects on human and animal health [2].

Aspergillus sp. and *Penicillium* sp. are the typical fungi species grown on stored rice. Xerophilic fungi, such as *Aspergillus* (*A. flavus*, *A. candidus*, *A. fumigates*) and *Penicillium* spp., are relatively tolerant to lower relative humidity than field fungi, thus their growth and development are improved during the

storage period [2]. Moreover, the parboiling process of rice makes them more susceptible to mycotoxigenic fungi, because of steeping of rice during the parboiling provides ideal conditions for the growth of mycotoxigenic fungi during the storage period [3]. The growth of these fungi is associated with the production of mycotoxins, which have adverse health effects on humans and animals [2]. The major aflatoxins produced by *A. flavus* are aflatoxin B1 and B2 (AFB1 and AFB2), among them aflatoxin B1 is considered as the most toxic and has mutagenic, immunosuppressive and teratogenic properties and also classified as Group 1A human carcinogen by the WHO-International Agency of Research on Cancer [4,5].

Synthetic pesticides have been efficient in controlling stored rice pests such as fungi, insects, rodents and nematodes [6]. However, the continuous use of pesticides causes development of resistant pest varieties, is harmful to the environment and humans and toxic to non-target species. Furthermore, the majority of chemical pesticides are tolerant to biodegradation, hence

cause pollution of soil and groundwater. The finding of safer alternatives for synthetic chemical pesticides has gained much attention [7].

Essential oils are complex volatile organic compounds synthesized in different plant species which show antibacterial, antifungal, anticarcinogenic and antioxidant properties. Cinnamon oil (CNO) is an essential oil obtained from *Cinnamomum zeylanicum* L. which is rich in cinnamaldehyde, linalool, β -caryophyllene and other terpenes. CNO has shown antifungal activity against *A. flavus*, *A. parasiticus*, *A. ochraceus* and *F. moniliforme* [8]. Lemongrass oil (LGO) is obtained from *Cymbopogon citratus*, which have been used as a traditional medicine in many countries. Also it has shown antifungal activity against *A. niger*, *A. fumigatus* and *A. flavus* [9]. Therefore, essential oils will be a promising alternative to chemical fungicides. But direct application of essential oils to control fungal growth has several limitations such as loss of antifungal activity due to volatilization, degradation of active compounds due to heat, oxygen and UV light, imparting unpleasant taste and aroma in food commodities [10].

Microencapsulation is a suitable method to overcome these drawbacks of the direct application of essential oils. This method involves the entrapment or coating of solid, liquid or gas particles of micron-sized within a wall material, usually a polymer. The resultant product of this technique is called microcapsules or microparticles. Encapsulation protects the active ingredient from the external environment, masking the colour, odour and taste facilitating the controlled release of the core material, ease of handling due to solid-state and allows safe handling of hazardous substances [11]. Several studies have shown the antimicrobial properties of microencapsulated essential oils. Microencapsulated coriander oil within β -cyclodextrin showed potential antifungal activity against *Aspergillus niger* and *Penicillium glaucum* with retaining the 41-46% of antifungal activity of free coriander oil. Also microencapsulated coriander oil showed antibacterial activity against both Gram-positive and Gram-negative bacteria such as *Listeria innocua*, *Achromobacter denitrificans*, *Shewanella putrefaciens*, *Enterobacter amnigenus* and *Pseudomonas fragi* with the MIC ranging from 10-20 mg/mL [12].

Among myriad of antifungal targets, components that make up the fungal cell membrane have been extensively studied as potential antifungal targets in inhibiting the growth of *A. flavus* using many plants derived compounds [13]. A fungal cell membrane consists of three main lipid components, which are sterols, sphingolipids and glycerophospholipids. However, as the most abundant sterol in the fungal cell membrane, ergosterol biosynthesis pathway is extensively used in experiments in identifying antifungal potential of substances. In fact, it is one of the most important biosynthesis pathways targeted by antifungals due to its importance in regulating the membrane fluidity and permeability and providing structural stability to the membrane [14]. Ergosterol biosynthesis is a high energy consuming pathway which requires the action of 25 different enzymes in the conversion of squalene to ergosterol [15]. While multiple targets can be identified in this pathway, in the current study squalene epoxidase, which is the enzyme responsible for the conversion

of squalene to lanosterol is sought for its ability to serve as a target in inhibiting *A. flavus* using cinnamon oil.

Not only in fungi but in all species that has chitin in their cell wall, chitin synthases (CHS; EC 2.4.1.16) plays a crucial role as a catalyst to the chitin synthesis pathway. Chitin synthase enzymes are categorized into seven classes however, each and every one of their exact roles are unknown. The chitin synthases expression and activity are clearly regulated throughout the fungal cell cycle and because of their abundance in fungal pathogens it has also been the most attractive target in antifungal development studies [16]. The substrate of the enzyme, uridine diphosphate-N acetylglucosamine (UDPGlcNAc) helps in making chitin chains required for the fungal cell wall assembly. In order to disrupt this activity of the enzyme, which then disrupts its cell wall synthesis, we focused on targeting CHS using ligands in cinnamon essential oil [17].

Genomic data of *Aspergillus* DNA has been arranged into eight chromosomes and aflatoxin producing genes are carried by the 3rd chromosome in its 54th cluster, which consist of 30 genes to be exact [18]. In its 75 kbp gene cluster the role of each protein and gene is maintained and from those gene products nor-1, vbs and amt-1 are the focus of the current *in silico* assessment of predicting the potential anti aflatoxigenic activity of cinnamon essential oils against *A. flavus* [19].

Previously reported the antifungal and anti-aflatoxigenic studies of plant essential oils against *A. flavus* have been mainly conducted under *in vitro* conditions. The most extensively studied plant-based compounds and essential oils against *A. flavus* and aflatoxin contamination in food products are sourced from flavour-enhancing plants like clove, cinnamon, oregano and thyme [20]. Furthermore, *in vitro* antifungal activity of cinnamon oil loaded chitosan microcapsules (CNO-CS-MCs) and lemongrass oil loaded chitosan microcapsules (LGO-CS-MCs) against *A. flavus* has been reported [21]. However, the limited availability of *in vivo* and *in situ* studies on their effects has significantly hindered their utilization in producing novel fungicides of natural origin [20]. Hence, herein, we extended our analysis to determine the *in vivo* and *in silico* antifungal activity of cinnamon leaf oil and lemongrass oil containing chitosan microcapsules.

EXPERIMENTAL

Paddy samples (Bg-11-11) were sourced from the Rice Research Institute, Bathalagoda, Sri Lanka. The husk was removed by using the mortar and pestle. Cinnamon leaf oil (CNO) and lemongrass oil (LGO) were acquired from the local market. Chitosan (medium molecular weight with the viscosity of 36.5 cps was obtained from Biotech Surinodo, Indonesia). Acetic acid (molecular weight of 60.05 g/mol with 99.5% assay) was purchased from Sigma-Aldrich, USA.

Gas chromatography-mass spectrometry (GC-MS) analysis of CNO and LGO: The GC analysis of oils was done by GC-MS (7890B-5977B, Agilent, USA) using a HP-5ms ultra inert column (dimensions 30 m \times 250 μ m \times 0.25 μ m). Helium was used as the carrier gas at a flow rate of 1 mL/min. The oven temperature was maintained at 70 $^{\circ}$ C for 1 min and programmed to 150 $^{\circ}$ C at a rate of 10 $^{\circ}$ C/min and held for 3 min,

increased to 200 °C at 5 °C/min and held for 3 min and increased to 250 °C at rate of 10 °C/min and held for 5 min. The MS source was established at temperature 230 °C and the maximum temperature was set to 250 °C, the quadrupole rod temperature was employed at temperature 150 °C and the maximum temperature was set to 200 °C. All the volatile constituents were identified by matching the obtained mass spectra with the standard mass spectra provided by the W9N11.L database.

Fabrication of CNO-CS-MCs and LGO-CS-MCs using ionotropic gelation method: In this study, microcapsules (MCs) were developed using the previously optimized formula by Subashinghe *et al.* [22]. Briefly, CNO (3 g) was added dropwise to a chitosan solution (1%, 100 mL) at room temperature with gentle stirring (200 rpm) using an overhead stirrer (IKA RW 20 digital). The mixture was homogenized at high speed (1000 rpm) for 10 min to obtain a good emulsion. Then the agitation speed was decreased to 200 rpm followed by the addition of sodium tripolyphosphate (0.5%) dropwise until a sufficient yield of MCs was observed under the light microscope. The solution was stirred for further 30 min at the same speed for the hardening of MCs. The solution obtained was subjected to centrifugation at 6000 rpm for 15 min. The supernatant was removed and the pellet was rinsed with Tween 80 (0.1% w/v). Then microcapsules were air-dried and stored in the refrigerator.

Determination of loading capacity of CNO-CS-MCs and LGO-CS-MCs: The loading capacity of oil-loaded MCs was performed using the method of Subashinghe *et al.* [22]. A concentration series of CNO and LGO (1-20 mg/100 mL) in Tween 80 solution (0.1% w/v) were separately prepared. Then the wavelength with the maximum absorption (λ_{\max}) was determined by scanning the solution with the highest concentration of oil at the wavelength range of 200-400 nm using UV-visible spectrometer (Orion AquaMate 800 UV-Vis). The calibration curves of CNO and LGO oil were made by plotting the absorbance values at λ_{\max} against the concentration of oil. A measured amount of oil-loaded MCs (1 g) was crushed using a mortar and pestle, then transferred to a volumetric flask with Tween 80 (0.1%, 100 mL). The resultant solution was kept overnight and then the absorbance was measured at the wavelength of 280 nm. The oil load of MCs was determined according to the following equation:

$$\text{Loading capacity (\%)} = \frac{W_o}{W_{mc}} \times 100$$

where W_o = weight of oil in known weight of MCs, W_{mc} = weight of microcapsules.

Isolation of *A. flavus*: An old rice sample (stored grains) was surface sterilized by soaking in a sterilized sodium hypochlorite (5%) solution for 2 min. Then rice grains were washed with sterilized distilled water for several times and placed on the sterilized tissue papers inside the biosafety cabinet for air drying. Then five dried rice grains were placed per petri dish, containing sterilized potato dextrose agar medium supplemented with chloramphenicol (10 µg/mL). The sealed Petri dishes were placed in an incubator at room temperature for 7 days. After the incubation period, fungal colonies that devel-

oped on the PDA media were transferred onto fresh PDA media to obtain pure cultures.

Characterization and identification of *A. flavus*: The morphological characteristics and microscopic features of pure cultures were observed under the light microscope. Then fungal colonies with putative morphological characteristics as *A. flavus* were selected and DNA sequencing was done using MACROGEN sequencing technology at Genetech, Sri Lanka. The DNA sequences were manually edited using BioEdit sequence alignment editor and compared with DNA sequences available in GenBank using Basic Local Alignment Search Tool (BLAST).

In vivo assay of CNO-CS-MCs and LGO-CS-MCs against *A. flavus* on stored rice: Rice grains were examined visually for mechanical damages and spoilage. Disinfection of rice grains was done according to the method described by Seepe *et al.* [23]. Healthy grains were soaked in sodium hypochlorite (3.5%) for 10 min followed by rinsing with sterilized distilled water for several times. Then grains were sprayed with ethanol (70% v/v) followed by rinsing with sterilized distilled water for several times and placed on a sterilized paper towel inside the biosafety cabinet for drying. The spore suspension of *A. flavus* was prepared by flooding a saline solution (1%, 10 mL) over a week-old pure culture of *A. flavus* in PDA media.

Disinfected dried rice grains (100) were added to each sterilized petri dish and inoculated with spore suspension (1 mL, 2×10^7 spores/mL) of *A. flavus*. Inoculated rice grains were placed inside the biosafety cabinet for air drying. Then different amounts of free oil and microcapsules containing different amount of each oil were mixed with inoculated rice grains and incubated at room temperature for 7 days. After the incubation, the minimum inhibitory dose of oil-loaded MCs and free oil was determined by detecting the petri dish with no visible growth of *A. flavus* on rice grains. A commercial fungicide, carbendazim was used as the positive control and empty MCs were used as the negative control for MCs-treated rice gains. Sterilized distilled water served as the negative control for free oil-treated rice grains. Each treatment was triplicated.

In order to determine the minimum lethal dose, rice grains in petri dishes with no visible growth in the previous assay were selected. Rice grains in each petri dish were placed on fresh PDA containing petri dish and incubated at room temperature for 7 days. Minimum lethal dose was determined by detecting the petri dish with no growth revival of *A. flavus* after 7 days of incubation.

Ligands preparation: Possible ligand molecules in CNO (eugenol, benzyl benzoate and β -caryophyllene) were identified by GC-MS analysis. Based on the ligands recognized, 3D structures of ligands were obtained from the PubChem database in SDF. The geometry optimization of each ligand molecule was performed by using Avogadro software using Force Field MMFF94, algorithm steepest descent, 500 steps. After the PDF format of each file was subjected to AutoDock Tools 1.5.6 and converted in to PDBQT format.

Protein preparation: Protein preparation was done according to the method described by Hansini *et al.* [24]. Homology modeling approach was utilized to create 3D models of the target proteins in the absence of crystal structures for the receptor-

ligand complexes for the target proteins. The amino acid sequences of certain suspected proteins from *A. flavus* were acquired from the NCBI database corresponding to the accession numbers of EED51173 (nor-1), EED51156 (omt-1), EED51154 (vbs), B8NYW4 (chitin synthase) and B8NFA6 (squalene epoxidase) in FASTA format. The FASTA sequence of each protein was inserted into the BLAST server and SWISS-MODEL server to find out suitable templates. The templates which had the highest coverage, highest GMQE (Global Model Quality Estimation) were selected and the proteins were modeled *via* SWISS-MODELER. The energy optimization of the modeled proteins was done by Galaxy Refine webserver.

Model validation: The model proteins were validated using Verify 3D, ERRAT, PROCHECK *via* SAVES v6.0 server and ProSA server.

Binding site identification: Binding pockets of each protein was identified by using Computed Atlas of Surface Topography of protein (CASTp) server.

Molecular docking: Molecular docking was done using the method described by Hansini *et al.* [24]. Both pdbqt. files of ligands and proteins were subjected to the AutoDock Tool 1.5.6. Grid parameter files were generated *via* Autogrid 4.2, while the Docking parameter files were generated by using AutoDock4.2. The settings of the Lamarckian genetic algorithm (LGA) were adjusted as number of genetic algorithms (GA) runs: 100, size of the population: 300 and 25000000 of maximum evaluations. Other parameters were kept as default. Both blind and site-specific dockings were performed.

Analysis of docking results: To visualize the binding conformations of each protein and ligands, Pymol software, Discovery Studio Visualizer and ligplot plus online server were used while protein ligand interaction profiler was used to validate the binding residues obtained from the pymol.

Molecular dynamic simulation: Molecular dynamic simulation was performed according to the method described by Hansini *et al.* [24]. Protein-ligand complex with the best negative binding energy was selected to perform molecular dynamics (MD) simulation. Molecular dynamics simulations was carried out using GROMACS (version 2021.4) software package, with force field of CHARMM36 and default water model of TIP3P. The protein-ligand complex was assigned center of the dodecahedron box with a minimum distance of 1.0 nm between complex and each side of the box. The ligand topology was prepared help of CHARMM General Force Field server. The LINCS bond length constraint algorithm and Particle Mesh Ewald summation were used to constraint bond lengths and for the electrostatic interactions and grid spacing of 0.12 nm combined with an interpolation order of 4 was used for long-range interactions. A cut-off of 1.4 nm was used for van der Waals interactions. Energy minimization was performed with help of steepest descent algorithm. The system was gradually heated up to 300 K throughout a 100 ps simulation time. Finally, the molecular dynamics production run was done in NPT ensembles at 300 K using V-rescale thermostat and at 1 bar using Berendsen barostat. Simulation results were obtained after 10 ns production runs with 2 fs time steps. Molecular dynamics simulation generated trajectory was used to obtain

the root mean square deviation (RMSD), radius of gyration (Rg) and root mean square fluctuation (RMSF).

RESULTS AND DISCUSSION

GC-MS analysis of CNO and LGO: The GC-MS analysis found total of 25 compounds in CNO. The major compounds present in CNO were found as eugenol (56.49%), β -caryophyllene (9.03%) and benzyl benzoate (8.43%), whereas in LGO the major constituents were *cis*-citral (36.26%) and *trans*-citral (45.55%).

Fabrication of CNO-CS-MSs using ionotropic gelation method: CNO-CS-MCs and LGO-CS-MCs were synthesized at previously optimized conditions. (MCs have been spherical in shape and polydispersed in the range of 100-1000 nm [22]).

Isolation and identification of *A. flavus* from stored rice: The isolated fungus was identified to be *A. flavus* based on the morphological and microscopic characteristics [25] and DNA sequencing. The ITS sequence of the isolated fungus was matched with the *A. flavus* sequence (accession number CP051033.1) from GenBank with 96.74% sequence identity.

Determination of minimum inhibitory dose against *A. flavus*: The antifungal activity of CNO-CS-MCs and LGO-CS-MCs was evaluated under *in vivo* conditions. The growth inhibition of *A. flavus* on rice was dose dependent. Rice grains treated with LGO-CS-MCs and CNO-CS-MCs showed complete inhibition of the fungus at LGO \geq 7.5 mg and CNO \geq 5 mg in respective MCs. Therefore, the minimum inhibitory doses of LGO-CS-MCs and CNO-CS-MCs were determined as 7.5 mg and 5 mg, respectively. The minimum inhibitory doses of free LGO and free CNO were determined as 1 mg and 2 mg, respectively. According to the results (Table-1), the antifungal activity of both LGO and CNO has reduced after the microencapsulation (the percentage inhibition of the fungus by MCs containing 1mg of LGO and 2 mg of CNO were 0% and 8.67%), which supports the slow release of oil through pores on the walls of microcapsules.

TABLE-1
PERCENTAGE INHIBITION OF *A. flavus* IN RICE TREATED WITH CNO, CNO-CS-MCs, LGO AND LGO-CS-MCs

Amount of oil (mg)	Inhibition (%)			
	CNO		LGO	
	Free CNO	CNO-CS-MC	Free LGO	LGO-CS-MC
1	81.67 \pm 3.06 ^a	0.00 \pm 0.00 ^b	100 \pm 0.00	0.00 \pm 0.00 ^a
2	100 \pm 0.00	8.67 \pm 1.53 ^b	100 \pm 0.00	5.33 \pm 0.58 ^b
3	100 \pm 0.00	22.33 \pm 2.08 ^c	100 \pm 0.00	20.67 \pm 1.15 ^c
4	100 \pm 0.00	64.67 \pm 2.52 ^d	100 \pm 0.00	44.67 \pm 2.08 ^d
5	100 \pm 0.00	100 \pm 0.00	100 \pm 0.00	74.33 \pm 2.52 ^c
7.5	100 \pm 0.00	100 \pm 0.00	100 \pm 0.00	100 \pm 0.00
10	100 \pm 0.00	100 \pm 0.00	100 \pm 0.00	100 \pm 0.00

*Mean of three replicates (n = 3). Data are presented as mean \pm standard deviation. Mean followed by different letters in superscript are significantly different from each other (ANOVA, Tukey's test, $p < 0.05$).

Determination of minimum lethal dose against *A. flavus*: Rice grains treated with 2, 3 and 4 mg of free CNO and 1-35 mg of free LGO in the minimum inhibitory dose assay did not show

any visible growth of fungus on rice grains. But after the incubation of those rice grains in PDA media, the growth of the fungus was observed. It indicated that fungus in treatments of 2, 3 and 4 mg of free CNO and 1-35 mg of free LGO in the previous assay only inhibited the growth of the fungus but not killed. But the treatments, 5 mg of CNO and above and 40 mg of LGO and above did not show growth of fungus after the incubation in PDA indicating that these amounts of CNO and LGO are fungicidal. Therefore, the minimum lethal dose of free CNO and free LGO against *A. flavus* was decided as 5 mg and 40 mg.

Treatments of rice grains with CNO-CS-MCs containing 5, 7.5 and 10 mg of CNO showed fungal growth revival in PDA media after 7 days of incubation. Whereas CNO-CS-MCs containing 12.5 mg of CNO and above did not show any growth revival of fungus in PDA media indicating that these amounts are fungicidal against *A. flavus*. Therefore, the minimum lethal dose of treatment with CNO-CS-MCs was decided as 12.5 mg. The minimum lethal dose of LGO-CS-MCs was not evaluated, because the fungal growth revival in PDA media was observed even at the MCs containing the highest LGO amount (70 mg).

Protein models validation: All the models of proteins were subjected to ERRAT, VERIFY 3-D, PROCHECK and ProSA servers after the energy minimization step *via* the Galaxy-Refine web server. The idea of the VERIFY 3-D is comparing of an atomic 3D structure with its corresponding 1D peptide sequence by deciding the structural class. A good model should have an 80.0% overall quality. When concerning the analyzed proteins, the overall quality diversified between 52% to 88%. The statistical details of non-bonded interactions between different atoms are given by the ERRAT server. If some model has the ERRAT score greater than the 60, it will consider as a good model. When analyzing the results of the ERRAT server, the values were within the range of 86% to 94%. The overall stereochemical quality and the arrangement of amino acids in allowed and forbidden regions are given by the PROCHECK. The possible Psi and Pi angles for amino acids could be obtained through the Ramachandran plot. The amino acids in all the selected proteins were in the most favoured region and as a percentage it was more than 90. The possible errors of the 3D structures of the proteins are detected by the ProSA web server. The total quality of the built model could be determined *via* the Z-score of the server. As well as, it gives the energy of the

protein with respect to the free random conformations of the proteins. The negative value of the ProSA web server illustrates the protein validity. The Z scores of analyzed proteins were assorted from -4.94 to -11.64. The all the results are illustrated below (Table-2).

Molecular docking analysis: In the practical component of this study, lemongrass and the cinnamon oil were used to check the inhibition capacity and visible that the cinnamon oil had the potential of causing significant impact on the growth of *A. flavus* compared to lemongrass oil. Therefore, this result was further confirmed by the docking analysis. Even though, cinnamon oil comprised of high fraction of eugenol according to the GC-MS analysis, the higher binding energies were appeared for benzyl benzoate and β -caryophyllene ligands which contained in fewer percentages in the cinnamon oil. The binding pocket of each protein was identified by using the CASTp web server and the docking was performed to the predicted binding pockets for all proteins. When concerning the results of the above (Table-3), the highest binding energy (-7.70 kcal/mol) was observed between squalene epoxidase enzyme and the benzyl benzoate ligand and the stability of the resultant protein-ligand complex was evaluated *via* molecular dynamic simulations. Squalene epoxidase is a key enzyme in the ergosterol biosynthesis pathway, where it converts the squalene to lanosterol and chitin synthase is crucial for the cell wall synthesis of *A. flavus*. Thus, due to the strong interactions of two enzymes with the analyzed ligands, the metabolism of fungi could be interrupted and the fungi could die. In addition to that gene products called vbs, omt-1 and nor-1, which are involved in the biosynthesis of aflatoxins in *A. flavus* could have affected by the ligands due to their high binding capability to the binding pockets of the gene products. Due to those facts, the growth of fungus and its ability to produce aflatoxins will be severely affected. The additional interaction details such as H-bonding were revealed by using protein ligand interaction profiler (Table-4). 2D and 3D visualizations of LigPlot server (Fig. 1a) and Discovery studio visualizer (Fig. 1b) were depicted below for the benzyl benzoate-squalene epoxidase complex.

Proteins and ligands interactions analysis: Amino acids involved in ligand-protein interactions for binding energies greater than (-6.00 kcal/mol)) including the types of interactions that each amino acid favours (Table-4).

TABLE-2
MODELED PROTEINS VALIDATION RESULTS

Model description		Chitin synthase	Nor1	Omt 1	VBS	Squaline epoxidase
Ramachandran plot	Residues in most favoured regions [A, B, L]	544 (94.1%)	201 (91.8%)	284 (91.9%)	440 (90.5%)	281 (90.9%)
	Residue in additional allowed regions [a,bl,p]	28 (4.8%)	16(7.3%)	24 (7.8%)	41 (8.4%)	26 (8.4%)
	Residues in generously allowed regions [-a, -b, -l, -p]	4 (0.7%)	1 (0.5%)	1 (0.3%)	2 (0.4%)	1 (0.3%)
	Residues in disallowed regions	2 (0.3%)	1 (0.5%)	0 (0%)	3 (0.6%)	1 (0.3%)
	Number of non-glycine and non-proline residues	578	219	309	486	309
	Number of end-residues (excl. Gly and Pro)	2	2	2	1	2
	Number of glycine residues	45	16	28	51	28
	Number of proline residues	23	11	26	33	26
	Total number of residues	648	248	365	571	365
	ERRAT overall quality score	94.618	87.7193	90.98	86.355	87.85
VERIFY 3-D (3D-1D score >0.2)	52.31%	50.81%	74.25%	88.62%	70.96%	
ProSA Z-score	-4.94	-7.32	-8.69	-11.64	-8.81	

TABLE-3
DOCKING RESULTS OF CRYSTAL STRUCTURES OF
FUNGAL PROTEINS WITH CINNAMON OIL LIGANDS

Protein	Phytochemicals	Binding energy (kcal/mol)
Squalene epoxidase	Benzyl benzoate	-7.70
	β -Caryophyllene	-6.67
	Eugenol	-5.81
Chitin synthase	Benzyl benzoate	-7.01
	β -Caryophyllene	-7.16
	Eugenol	-5.87
Nor-1	Benzyl benzoate	-6.64
	β -Caryophyllene	-6.28
	Eugenol	-5.05
Vbs	Benzyl benzoate	-7.24
	β -Caryophyllene	-6.88
	Eugenol	-5.60
Omt-1	Benzyl benzoate	-7.47
	β -Caryophyllene	-7.63
	Eugenol	-5.61

Molecular dynamics results: The molecular dynamics simulations measure particle interactions as a function of their individual molecule particles' coordinates. Molecular dynamics simulation is used to analyze the behaviour of a protein and its ligand over a particular time period. Molecular dynamics is useful for measuring protein flexibility. A time step smaller than the fastest movement, must be used to accurately characterize molecular motion. The 2 fs time step is commonly used since the fastest vibration of a hydrogen atom is approximately 13 fs (1 femtosecond = 10^{-15} seconds). In this study, most of the attention is paid to determine parameters of the radius of gyration (Rg), root mean square deviation (RMSD) and root mean square fluctuation (RMSF).

Radius of gyration (Rg): A rigid body's gyration radius is a geometric characteristic and consider the center of mass. It's the same as the body's actual mass distribution. If the body's total bulk is concentrated. This theory further applies for the analyzing the protein-ligand complex. Because of that,

TABLE-4
INTERACTION OF LIGAND-PROTEIN[†] AND THEIR BINDING ENERGIES DATA

Protein	Phytochemicals	Binding energies (kcal/mol)	Amino acids responsible for ligand-protein interactions
Squalene epoxidase	Benzyl benzoate	-7.70	Glu70, Leu71, Phe100, Tyr239*, Gln240
	β -Caryophyllene	-6.67	Pro299, Arg323, Pro325
Chitin synthase	Benzyl benzoate	-7.01	Tyr460*, Leu461, Glu463, Asn509, Asp715, Trp718, Tyr784*, Lys318
	β -Caryophyllene	-7.16	Val547, Phe551, Phe554, Tyr820, Ile823, Ile824
nor1	Benzyl benzoate	-6.64	Thr117, Phe119, Gln217, Gly221 [‡] , Arg226
	β -Caryophyllene	-6.28	Ile36, Pro167, Ile168, His215, Val216
VBS	Benzyl benzoate	-7.24	Ile394, Tyr577, Tyr578, Ala172 [‡] , Tyr470*
	β -Caryophyllene	-6.88	Tyr158, Gln160, Tyr578, Ala613, Val628
Omt-1	Benzyl benzoate	-7.47	Val235, Leu343, Asp345, Ile348, Trp400*, Lys402, Arg401 [#]
	β -Caryophyllene	-7.63	Leu343, Leu344, Trp382, Ile386, Thr395, Ile398

[†]Each interaction is represented by hydrophobic interactions, hydrogen bonding[‡], hydrophobic interactions + H bonding, salt bridge, π stackings^{*}, salt bridge + H bonding[#] and hydrophobic + π stackings^{*}, respectively.

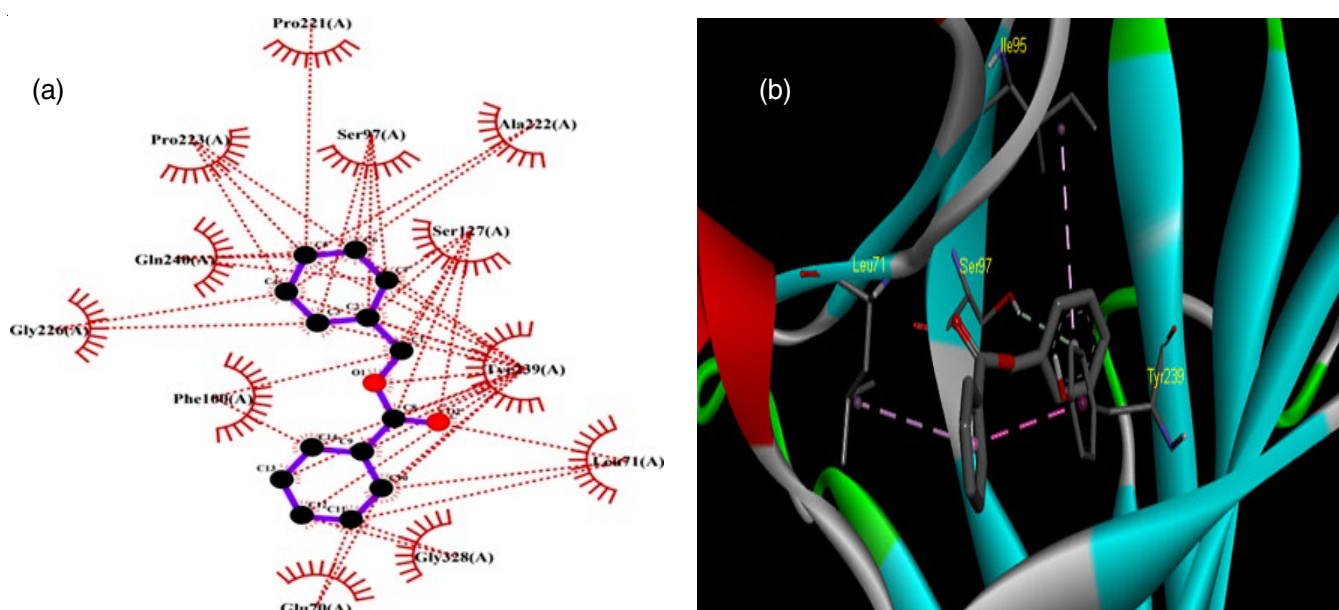


Fig. 1. 2D and 3D visualization of protein-ligand complex of benzyl benzoate-squalene epoxidase

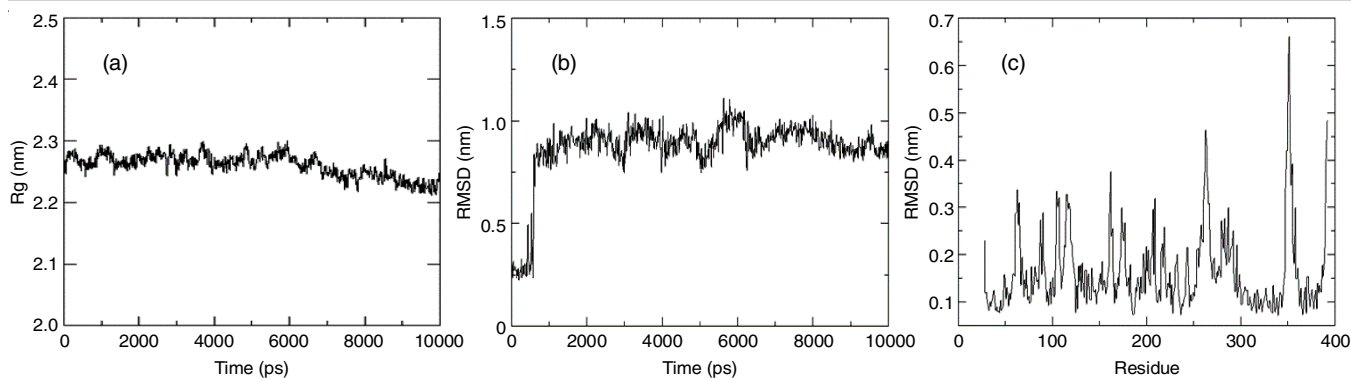


Fig. 2. (a) Radius of gyration (Rg) plot of SQ-BEN complex, (b) root mean square deviation (RMSD) plot of the SQ-BEN complex, (c) root mean square fluctuation (RMSF) plot of SQ-BEN complex

Rg was used to determine the size and structural flexibility of the protein-ligand complex to explain how the protein-ligand complex structure compactness changes over time in a simulation period. According to the Rg plot of SQ-BEN complex (Fig. 2a), a flat curve between ~ 0.20 nm and ~ 0.30 nm represented the stabilization of SQ-BEN complex during the simulation time frame of 10 ns.

Root mean square deviation (RMSD): Root mean square deviation is used to study conformational similarities and the stability of the protein-ligand complexes. The RMSD is determined by rotating and converting the instantaneous structures' coordinates. After that it is superimposed with the reference initial structure which has greatest overlap. Considering the information, which generates *via* RMSD calculation, explains the system flexibility, whether is it in the equilibrium or have any conformational changes. According to the SQ-BEN complex RMSD plot analysis (Fig. 2b), leveling off just under ~ 0.10 nm indicated its stability throughout the 10 ns of whole simulation time.

Root mean square fluctuation (RMSF): RMSF is a numerical measurement, which is like the RMSD. RMSF calculates the flexibility of the residues or the movement of the residues during the whole simulation time. The plot generated as RMSF per residue *vs.* residues number. Based on the RMSF plot analysis (Fig. 2c), the responsible protein residues were identified, which were involved in the molecular motion. If molecule shows higher movement indicates that it has higher flexible ability. Due to the higher flexibility, those residues could more contribute for the protein-ligand interactions like, H-bonds and hydrophobic interactions. The residues which have significant intense fluctuation peaks may not contribute to the interactions due to the initiating the local changes of the protein (SQ) structure. According to the RMSF graph of SQ-BEN complex (Fig. 2c), significant fluctuation peaks above ~ 0.25 nm explains that, non-involvement of ligand (BEN) for the complex formation but fluctuations between ~ 0.10 nm and ~ 0.15 nm residues represented that, feasibility of the interactions with protein (SQ) and ligand (BEN).

Conclusion

Both microencapsulated cinnamon leaf oil (CNO) and lemongrass oil (LGO) showed antifungal activity against *A. flavus*. Microencapsulated CNO and LGO are fungistatic at 5

mg and 7.5 mg, respectively, whereas the microencapsulated CNO is fungicidal at 12.5 mg. According to the results, CNO-CS-MCs exhibited greater antifungal activity against *A. flavus* in stored rice compared to LGO-CS-MCs. The microencapsulation of CNO and LGO reduces their antifungal activity and it indicates the controlled release of oil from microcapsules. Eugenol, benzyl benzoate and β -caryophyllene phytochemicals were computationally investigated for selected enzymes and proteins in *A. flavus*. Even though, cinnamon oil comprised of high fraction of eugenol according to the GC-MS analysis, the higher binding energies were appeared for benzyl benzoate and β -caryophyllene ligands which contained in fewer percentages in the cinnamon oil. The highest binding energy (-7.70 kcal/mol) was obtained for the SQ-BEN complex and it was further analyzed by molecular dynamics (MD) stimulations. According to the molecular dynamics stimulations for the SQ-BEN complex, a stable protein-ligand complex can be observed throughout the 10 ns of whole simulation time period. Based on the results, CNO-CS-MCs and LGO-CS-MCs show their antifungal potential to be used as a biopesticide against *A. flavus* in food industry.

ACKNOWLEDGEMENTS

This work was supported by University of Kelaniya under the research grant- RC/MDRG/2021/01.

CONFLICT OF INTEREST

The authors declare that there is no conflict of interests regarding the publication of this article.

REFERENCES

1. J.W.P. Kumari, L.K.W. Wijayarathne, N.W.I.A. Jayawardena and W.C.P. Egodawatta, *Sri Lankan J. Agric. Ecosyst.*, **2**, 99 (2020); <https://doi.org/10.4038/sljae.v2i1.32>
2. M. Mannaa and K.D. Kim, *Mycobiology*, **46**, 287 (2018); <https://doi.org/10.1080/12298093.2018.1505247>
3. J.M.R.S. Bandara, A.K. Vithanage and G.A. Bean, *Mycopathologia*, **115**, 31 (1991); <https://doi.org/10.1007/BF00436418>
4. S. Nayak, U. Dhua and S. Samanta, *Int. J. Curr. Microbiol. Appl. Sci.*, **3**, 170 (2014).
5. M. Mannaa and K.D. Kim, *Mycobiology*, **44**, 67 (2016); <https://doi.org/10.5941/MYCO.2016.44.2.67>

6. A. Sharma, V. Kumar, B. Shahzad, M. Tanveer, G.P.S. Sidhu, N. Handa, S.K. Kohli, P. Yadav, A.S. Bali, R.D. Parihar, O.I. Dar, K. Singh, S. Jasrotia, P. Bakshi, M. Ramakrishnan, S. Kumar, R. Bhardwaj and A.K. Thukral, *SN Appl. Sci.*, **1**, 1446 (2019); <https://doi.org/10.1007/s42452-019-1485-1>
7. G.M.W. Lengai, J.W. Muthomi and E.R. Mbega, *Sci. Afr.*, **7**, e00239 (2020); <https://doi.org/10.1016/j.sciaf.2019.e00239>
8. Y. Xing, X. Li, Q. Xu, J. Yun and Y. Lu, *Int. J. Food Sci. Technol.*, **45**, 1837 (2010); <https://doi.org/10.1111/j.1365-2621.2010.02342.x>
9. S. Ali and A. Yousef, *Int. J. Curr. Microbiol. Appl. Sci.*, **2**, 261 (2013).
10. E.A. Soliman, A.Y. El-Moghazy, M.S.M. El-Din and M.A. Massoud, *J. Encapsulation Adsorpt. Sci.*, **3**, 48 (2013); <https://doi.org/10.4236/jeas.2013.31006>
11. N.V.N. Jyothi, P.M. Prasanna, S.N. Sakarkar, K.S. Prabha, P.S. Ramaiah and G.Y. Srawan, *J. Microencapsul.*, **27**, 187 (2010); <https://doi.org/10.3109/02652040903131301>
12. N. Eghbal, W. Liao, E. Dumas, S. Azabou, P. Dantigny and A. Gharsallaoui, *Appl. Sci.*, **12**, 3837 (2022); <https://doi.org/10.3390/app12083837>
13. L. Tian, T. Qiang, C. Liang, X. Ren, M. Jia, J. Zhang, J. Li, M. Wan, X. YuWen, H. Li, W. Cao and H. Liu, *Eur. J. Med. Chem.*, **213**, 113201 (2021); <https://doi.org/10.1016/j.ejmech.2021.113201>
14. L.M. Douglas and J.B. Konopka, *Annu. Rev. Microbiol.*, **68**, 377 (2014); <https://doi.org/10.1146/annurev-micro-091313-103507>
15. S. Dhingra and R.A. Cramer, *Front. Microbiol.*, **8**, (2017); <https://doi.org/10.3389/fmicb.2017.00092>
16. M.D. Lenardon, C.A. Munro and N.A.R. Gow, *Curr. Opin. Microbiol.*, **13**, 416 (2010); <https://doi.org/10.1016/j.mib.2010.05.002>
17. F. Trail, P.K. Chang, J. Cary and J.E. Linz, *Appl. Environ. Microbiol.*, **60**, 4078 (1994); <https://doi.org/10.1128/aem.60.11.4078-4085.1994>
18. K.C. Ehrlich, *Toxins*, **1**, 37 (2009); <https://doi.org/10.3390/toxins1010037>
19. P.P. Singh, A.K. Jaiswal, A. Kumar, V. Gupta and B. Prakash, *Sci. Rep.*, **11**, 6832 (2021); <https://doi.org/10.1038/s41598-021-86253-8>
20. F. Tian, S.Y. Woo, S.Y. Lee, S.B. Park, Y. Zheng and H.S. Chun, *Antibiotics*, **11**, 1727 (2022); <https://doi.org/10.3390/antibiotics11121727>
21. Y.L. Paragodaarachchi, P. Subasinghe and S.R. Wickramarachchi, *Acta Chem. Iasi.*, **28**, 129 (2020); <https://doi.org/10.2478/achi-2020-0009>
22. U.G.P.P. Subasinghe and S. Wickramarachchi, *Ceylon J. Sci.*, **48**, 279 (2019); <https://doi.org/10.4038/cjs.v48i3.7652>
23. H.A. Seepe, K.E. Lodama, R. Sutherland, W. Nxumalo and S.O. Amoo, *Plants*, **9**, 1668 (2020); <https://doi.org/10.3390/plants9121668>
24. N. Hansini, A.M.S.C. Sooriyawansa, P.A.S.N.P. Jayawardena, P.G.J.D. Kumarathunga, P.D.H. Dananjaya, E.A.C.P. Edirisinghe, M.D.N. Alwis, D.A. Daranagama, J.N. Dahanayake and C.C. Kadigamuwa, *Med. Plants - Int. J. Phytomedicines Relat. Ind.*, **15**, 677 (2023); <https://doi.org/10.5958/0975-6892.2023.00068.0>
25. R. Khan, F. Mohamad Ghazali, N.A. Mahyudin and N.I.P. Samsudin, *Agriculture*, **10**, 450 (2020); <https://doi.org/10.3390/agriculture10100450>